

IP modeling and reservoir parameters prediction of tight sandstone in Zhongjiang gas field, Sichuan Basin

Liangjun Yan¹, Xiaolong Tong^{1*}, Kui Xiang¹, Xingbing Xie¹, Lei Zhou¹, Li Ma², Kefei Zhang²

¹Key Laboratory of Exploration Technologies for Oil and Gas Resources, Yangtze University, Ministry of Education, Wuhan, 430100, yljemlab@163.com

²SINOPEC Geophysical Research Institute Co.,Ltd. Nanjing, 211103

SUMMARY

The Sichuan Basin is rich in tight sandstone reservoirs with significant tight gas. However, due to their characteristics of low porosity, low permeability, and strong heterogeneity, conventional reservoir evaluation methods based primarily on resistivity struggle to accurately predict and assess the gas-bearing potential of these tight sandstone reservoirs. Conducting induced polarization (IP) modeling for tight sandstone is critically important for developing new methods of reservoir prediction and evaluation based on IP multi-parameters. Based on the measurements and the analysis of complex resistivity of tight sandstone samples in Zhongjiang gas field, Sichuan Basin, this paper adopted the MGEMTIP model suitable for tight reservoir to carry out IP modeling. A complex resistivity model of tight reservoir controlled by porosity, pore fluid salinity, clay content and saturation was constructed through mineral composition analysis, scanning electron microscopy and anisotropy testing, and the prediction methods of reservoir saturation and permeability were established, which provided a theoretical basis not only for the study of electromagnetic forward and inversion methods, but also for the unconventional reservoir prediction and evaluation.

Keywords: resistivity, chargeability, induced polarization, permeability, reservoir prediction

INTRODUCTION

The Sichuan Basin in China is endowed with abundant tight gas reservoirs. However, the exploration and evaluation of these reservoirs are challenging due to the low porosity, low permeability, strong heterogeneity, and complex pore structures of the reservoirs. Traditional seismic exploration methods fall short in meeting the high-precision exploration requirements for tight gas. The electrical properties of tight reservoirs exhibit significant changes with variations in fluid content. Therefore, studying electromagnetic (EM) exploration technologies based on multi-parameter electrical properties can reduce exploration and development costs and enhance the accuracy of comprehensive interpretation.

IP is a physical-chemical phenomenon caused by the change of electric double layer (EDL) structure at the interface between rock minerals and pore fluids driven by an external electric field. The mechanisms include complex processes such as ionic polarization, membrane polarization, and electrode polarization (Kemna A et al., 2012). Through comprehensive analysis of the mineral

composition and pore structure characteristics of the reservoir rocks the main process and influencing factors of low frequency polarization can be determined. The measurement of the dispersion curve of complex electrical resistivity of reservoir rocks and the study of the relationship between IP characteristic parameters and reservoir parameters based on complex electrical resistivity inversion are effective approaches for reservoir prediction. The Cole-Cole model qualitatively analyzed mineral composition and pore structure. However, due to the complexity of unconventional oil and gas reservoirs' mineral composition, pore structures, and pore fluids (multiphase flow), the Cole-Cole model is less applicable. The MGEMTIP model, based on the theory of equivalent medium, is better suited to represent the complex mineral-fluid compositions, adapt to anisotropy, and closely relate model parameters to the structure. This makes it more accurate in depicting the IP phenomena in unconventional reservoirs (Tong et al., 2020).

Saturation and permeability are critical parameters in evaluating oil and gas reservoirs. When reservoir pore fluid and porosity characteristics are favorable,

EMIW2024 abstracts are distributed under the Creative Commons Attribution 4.0 Unported License. Authors retain the copyright of the abstract but grant any third party the right to use the abstract freely as long as its original authors and citation details are identified.

To view a copy of this license, visit <https://creativecommons.org/licenses/by/4.0/>

the water saturation of the reservoir strongly correlates with resistivity, aligning with the Archie law. For tight reservoirs with low water saturation, the dielectric polarization frequency at mineral interfaces decreases, and the combined effects of IP and dielectric polarization become significant at higher frequencies. Under these conditions, the Archie formula needs to account for complex resistivity effects. Similarly, permeability prediction must consider IP influences. Research shows that IP parameters are sensitive to rock porosity, equivalent pore radius, and tortuosity. Thus, these parameters can be used to refine the Kozeny-Carman (K-C) model and establish a theoretical relationship between electrical parameters and permeability (Slater, 2007; Weller, 2019).

METHOD

Compared to the commonly used Cole-Cole model, GEMTIP (Zhadanov, et al., 2008) model's parameters are closely related to the physical structure of the rock. It better describes the IP response characteristics of oil and gas reservoirs, especially in representing multiphase media and electrical anisotropy. Considering the effects of boundary polarization, Tong and Yan (2020) revised the definition of effective conductivity in the GEMTIP model and proposed the modified GEMTIP (MGEMTIP) model. Under the assumption of a one-dimensional spherical perturbation, the model is:

$$\sigma_e(\omega) = \sigma_0 M_0 \left\{ 1 + \sum_l \eta_l [1 - 1/(i\omega\tau_l + 1)] \right\} \quad (1)$$

Where $M_0 = 1 - \sum_l 3f_l/2$ is the effective spatial fraction of the background medium, $\tau_l = a_l b_l (2\sigma_0 + \sigma_l) / 2\sigma_0 \sigma_l$ is the relaxation time corresponding to the perturbation body, $\eta_l = 9f_l \sigma_l / [(4\sigma_0 + 2\sigma_l) M_0]$ is the polarizability corresponding to the perturbation body, σ_0 is the conductivity of the background medium. For the l type of perturbation medium, the parameters are: $f_l, \sigma_l, \lambda_l, a_l$ are the volume fraction, the conductivity, the surface polarization factor and the equivalent sphere radius. It can be observed that significant polarization can only be detected when the conductivity of the perturbation body is relatively high compared to the conductivity of the background medium.

According to the Archie's law, the low-frequency conductivity of water-saturated rocks is given by:

$$\sigma_w(0) = \sigma_w \phi^m S_w^n = \sigma_w / F_w I_w \quad (2)$$

Where, σ_w is the conductivity of the pore fluid, F_w is the formation factor of the rock, I_w is the resistivity index, ϕ is the porosity, m is the cementation exponent. S_w is the water saturation, n is the saturation exponent. When IP occurs, the high-frequency conductivity results from the

combined conduction effects of the pore fluid and clay. Using equations (1) and (2), the conductivity of the rock containing unsaturated fluids can be derived as follows:

$$\sigma_e(\omega) = \frac{\sigma_w}{F_w I_w} + \frac{\sigma_H}{F_H I_H} \left[1 - \sum_{i=1}^N \left(\frac{g_i}{1 + i\omega\tau_i} \right) \right] \quad (3)$$

Where $\sigma_H = 9\sigma_w \sigma_c / (4\sigma_w + 2\sigma_c)$ is the high-frequency additional effective conductivity,

$F_H = 1 / \sum_l f_l = f^{-1} = f_c^{-m}$ is the relative proportion of

clay content, $g_i = f_i / f$ is the effective proportion of clay minerals at different scales, I_H is the resistivity index of the clay. Similar to the pore fluid conductivity, the conductive capacity of clay is also influenced by its fluid saturation state. The electrical properties of clays are affected by their interaction with fluids, which varies with saturation. The complex mechanisms of conductivity and polarization in unsaturated clay require calibration through experimental measurements to accurately characterize these effects.

K-C relationship can be used to establish a model for reservoir permeability. Given that the formation factor has a strong correlation with porosity, and that surface conductivity reflects the complexity of the pore space, a permeability relationship can be derived based on the saturation-dependent formation factor F_w and the normalized polarizability η_l . The relationship is expressed as follows:

$$k^* = \frac{\alpha}{\eta_l^\beta F_w^\gamma} \quad (4)$$

Where $\eta_l = \sigma_e(0)(\sigma_e(\infty) - \sigma_e(0)) / \sigma_e(\infty)$, α, β, γ are empirical constants that need to be calibrated through experimental measurements. The actual formation resistivity is in an unsaturated state. By applying model corrections, the resistivity and polarizability characteristics under saturated conditions can be obtained. Then, using equation (4), the permeability can be estimated.

EXPERIMENT CONDITIONS

50 samples were all from the Jurassic Shaximiao Formation of tight sandstone reservoir in the Zhongjiang gas field, including 30 cylindrical core samples, 10 cubic samples, and 10 well samples at depths ranging from 2400m to 2700m. Various conditions were applied to the core samples, including measurements of porosity, permeability, and complex resistivity. Three states for measuring porosity and permeability are normal temperature and pressure (25°C, 5MPa), simulated depth of 2000m (73°C, 21MPa), and simulated depth of 3500m (118°C, 37MPa). Five different states for complex resistivity measurement are normal temperature and pressure (25°C, 5MPa), and four

temperature-pressure states simulated from depths of 2000m to 3500m (73°C, 21MPa; 88°C, 26MPa; 103°C, 31MPa; 118°C, 37MPa). The pore fluid used was 5% saturated saline water, and the frequency range for complex resistivity testing was from 0.01Hz to 10kHz. Based on the measured complex resistivity curves and using equation (4) along with the Debye Decomposed (DD) algorithm, the IP parameters of resistivity and chargeability were estimated.

RESULTS AND DISCUSSION

Composition analysis (Figure 1) revealed that the low-resistivity minerals in the reservoir rocks are primarily clays, which are predominantly filling the intergranular pores of the clastic particles. The clay interfaces are complex, leading to poor connectivity of pore fluids. At high frequencies, conductivity is good, but at low frequencies, the impedance increases due to the formation of high-resistivity polarization bodies at the clay-fluid interface. This structure conforms to the model relationship corresponding to equation (3) and can be modeled using complex resistivity measurements of rock samples.

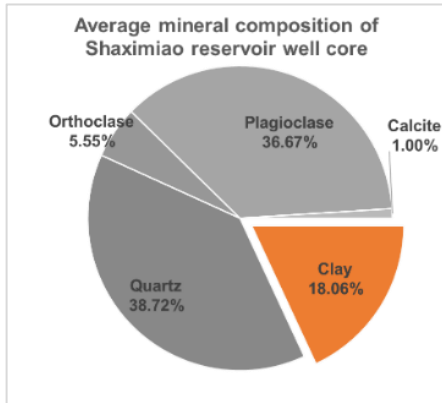


Figure 1. Average mineral composition of Shaximiao Formation of rock samples

The anisotropy measurement was conducted on 10 cubic samples. The anisotropy coefficients of dry resistivity, saline saturated resistivity, along with polarization and permeability were determined as 1.27, 1.14, 1.47, and 3.99, respectively. It is evident that the electrical anisotropy characteristics of the Shaximiao Formation are not significant, whereas the permeability shows strong anisotropy influenced by heterogeneity. Figure 2 illustrates a linear relationship in logarithmic coordinates between clay content and surface conductivity.

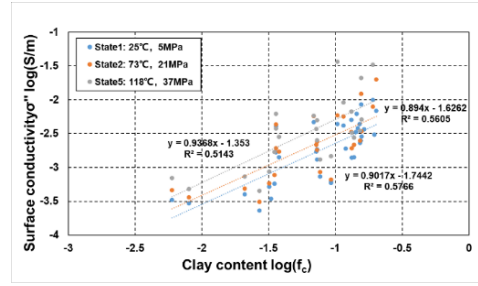


Figure 2. The relationship between clay and surface conductance at different states

The sandstone of the Shaximiao Formation generally conforms to the assumption of isotropic media dominated by pore fluid conductivity and clay mineral polarization. For different simulated burial depths, quantitative IP models for saturated water bearing samples can be established using formula (3), and the IP parameters of three states are shown in Table 1.

Tables 1. Parameters of induced polarization models under different depth conditions.

State	$\sigma_w/S/m$	$\sigma_c/S/m$	m	m'
1	8.00	0.0080	1.6172	0.9017
2	15.74	0.0105	1.4968	0.8940
5	22.94	0.0197	1.3673	0.9368

The model parameters I_w and I_H are calibrated using equation (3) and complex resistivity measurements of unsaturated rock samples. Through equation (2), the resistivity exponent of tight sandstone is determined to be $n = 1.6492$. Despite the complex factors affecting of I_H , it remains a function of water saturation, expressed as $I_H = 1/f(S_w)$, and the saturation ratio chargeability was defined as $\bar{\eta} = \frac{I_w}{I_H} = f(S_w)S_w^{-n}$. Figure 3 illustrates the relative polarization obtained under State 1 condition, showing a nonlinear relationship with S_w .

By curve fitting, the relationship between clay resistivity index and water saturation can be calculated.

$$I_H = (-24.132S_w^{4.6492} + 44.085S_w^{3.6492} - 22.794S_w^{2.6492} + 3.7717S_w^{1.6492})^{-1} \quad (5)$$

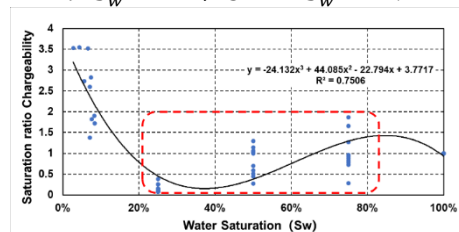


Figure 3. Nonlinear relationship between saturation ratio chargeability and saturation of cores under State1 condition

After obtaining I_w and I_H , a complex resistivity model for reservoir rock samples can be established. Figure 4 shows the variation of model resistivity and polarizability under different porosity conditions with changes in water saturation under State 1 conditions. The polarizability exhibits a nonlinear relationship with water saturation overall.

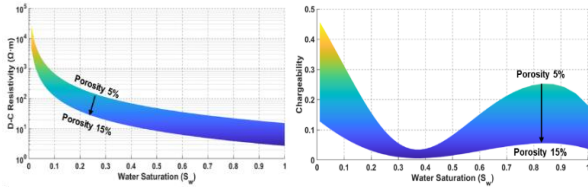


Figure 4. Shows the trend of model resistivity(left) and polarizability(right) with changes in porosity and water saturation under the condition of 18.6% clay content in State 1.

Although the Archie law provides an ideal relationship between resistivity and saturation, the chargeability is of great significance for estimating water saturation under unknown porosity conditions (e.g. saturation is lower when chargeability exceeds 25%, Figure 4). Considering the nonlinear relationship between water saturation and chargeability, based on the resistivity and chargeability of rock samples, intelligent algorithm was used to classify and predict saturation. Figure 5 shows the saturation estimated through Softmax classification and weighted estimation of samples under State 1 condition. Compared to prediction based solely on resistivity, the average relative error decreases from 22.86% to 11.41%.

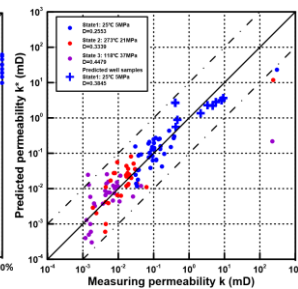
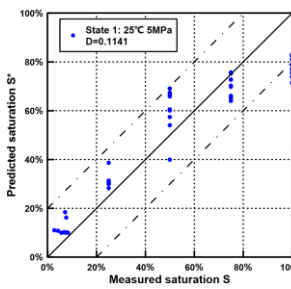


Figure 5. Saturation prediction result **Figure 6.** Permeability prediction result

According to equation (4), fitting was performed to estimate permeability under three different states, resulting in predictive models for permeability under corresponding state conditions:

$$\begin{aligned}
 \text{State 1: } k^*_1 &= 1.14 \times 10^7 m_t^{-2.4929} F_f^{-3.0477} \\
 \text{State 2: } k^*_2 &= 2.71 \times 10^4 m_t^{-1.1414} F_f^{-2.1927} \\
 \text{State 3: } k^*_3 &= 1.13 \times 10^5 m_t^{-1.2559} F_f^{-2.4860}
 \end{aligned} \quad (6)$$

Figure 6 depicts the permeability prediction results of rock samples under three different state conditions. Compared to predictions based solely

on resistivity, the average relative error in predictions decreased from 74.91% to 38.45%. Under actual geological conditions, well logging data can be used to estimate porosity and formation water salinity, and then intelligent algorithms can be applied to estimate rock saturation. Combining resistivity, polarizability, and permeability models under fully saturated conditions to achieve reservoir permeability prediction.

CONCLUSIONS

Through experimental analysis, it is hypothesized that the reservoir satisfies the advantages of electrical isotropy, pore fluid conductivity, and clay mineral induced polarization. Based on GEMTIP, a complex resistivity model for the Zhongjiang gas reservoir was established. The prediction of reservoir saturation and permeability was achieved using the results of complex resistivity experiments and intelligent prediction algorithms, providing experimental and theoretical basis for electromagnetic exploration methods to detect gas content in tight reservoirs.

ACKNOWLEDGEMENTS

This research was supported by the National Natural Science Foundation of China (42030805, 42204079, and 42174083).

REFERENCES

Kemna A, et al (2012) An overview of the spectral induced polarization method for near-surface applications. *Near Surface Geophysics* 10(6): 453-468.

Nordsiek S, Weller A (2008) A new approach to fitting induced-polarization spectra. *Geophysics* 73(6): F235-F245.

Slater L (2007) Near surface electrical characterization of hydraulic conductivity: From petrophysical properties to aquifer geometries—A review. *Surveys in Geophysics* 28: 169-197.

Weller A, Slater L (2019) Permeability estimation from induced polarization: an evaluation of geophysical length scales using an effective hydraulic radius concept. *Near surface geophysics* 17(6): 581-594.

Xiaolong T, Liangjun Y, Kui X (2020) Modifying the generalized effective-medium theory of induced polarization model in compacted rocks. *Geophysics* 85(4): MR245-MR255.

Zhdanov MS (2008) Generalized effective-medium theory of induced polarization: *Geophysics*, 73, 197-211.